Reports

Mantle Plume Mixing Along the Reykjanes Ridge Axis: Lead Isotopic Evidence

Abstract. *Gradients of lead isotopic ratios from basalts erupted along the Reykjanes Ridge and Median Neovolcanic Zone of Iceland confirm mantle plume mixing with the depleted asthenosphere along the ridge axis.*

Geochemical studies of basalts erupted along the Reykjanes Ridge and its extension over the Median Neovolcanic Zone of Iceland have revealed striking gradients in minor and trace element concentrations (*1*). These studies and other geophysical and morphological evidence in the area have given strong support to the mantle plume hypothesis (*2, 3*) and led Schilling (*1*) to suggest a model consisting of two mantle sources, a mantle plume rising beneath Iceland and a depleted low velocity layer beneath the ridge. Mixing of these two sources at mantle depth was assumed to be the cause of the gradients, particularly in the La/Sm ratio. A subsequent $^{87}\mathrm{Sr}/^{86}\mathrm{Sr}$ test of the model (*4*) supported the concept presented by Schilling, but also suggested a less regular mixing along the transitional zone than was apparent from the gradient in the La/Sm ratio.

Although challenged on various and debatable grounds (*5–8*), the binary mantle mixing model remains, we believe, the most important process in producing the gradients of large ionic lithophile (LIL) trace element ratios thus far observed along the Reykjanes Ridge–Iceland profile (*1, 9*). As further evidence in support of this model, we now present Pb iotopic compositions for 16 Reykjanes Ridge and 2 Iceland basalts, as well as Th, U, and Pb concentrations for 7 of these samples, whose locations are shown in Fig. 1.

Results. Table 1 shows the Pb isotopic data obtained in this study and Table 2 the U, Th, and Pb concentrations (*10, 11*). All basalts analyzed are very fresh, tholeiitic in composition, and vary from slightly quartz normative to olivine normative (*12*). Figure 2 shows the $^{206}\mathrm{Pb}/^{204}\mathrm{Pb}$ and $^{208}\mathrm{Pb}/^{204}\mathrm{Pb}$ ratios of these basalts with respect to their distance from the southern tip of Iceland. Data for three samples from Sun and Jahn (*13*) and one from Welke *et al.* (*14*), all from the Median Neovolcanic Zone of Iceland, are also plotted in Fig. 2. For comparison, $^{87}\mathrm{Sr}/^{86}\mathrm{Sr}$ and La/Sm ratios previously reported by Hart *et al.* (*4*) and Schilling (*1*), respectively, are also shown in Fig. 2.

The $^{206}\mathrm{Pb}/^{204}\mathrm{Pb}$ profile shows high values over Iceland and low values south of 61°N to the Gibbs fracture zone. In be-

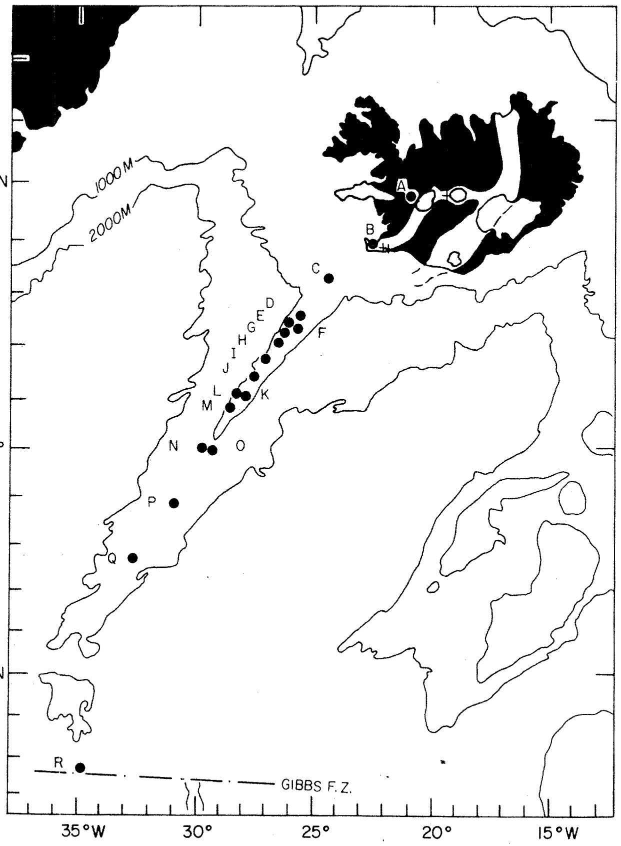

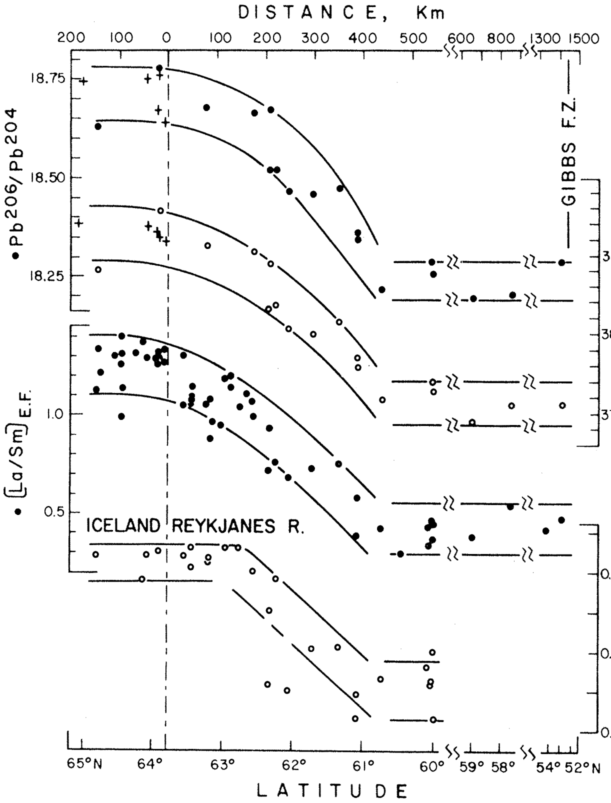

Fig. 1 (left). Map showing locations where basalts were obtained. Lead isotopic compositions were determined for all the samples and U, Th, and Pb concentrations for those from stations B, C, D, F, I, M, and N. Ridge basalts were dredged by the R.V. *Trident* during cruises TR41 and TR101 in 1967 and 1971. Letter codes are for reference with Tables 1 and 2. Crosses denote samples described in (*13*) and (*14*). Fig. 2 (right). Variation of $^{206}\mathrm{Pb}/^{204}\mathrm{Pb}$, $^{208}\mathrm{Pb}/^{204}\mathrm{Pb}$, $(\mathrm{La/Sm})_{\mathrm{EF}}$, and $^{87}\mathrm{Sr}/^{86}\mathrm{Sr}$ in basalts with latitude. Regular gradients are observed. Lead isotopic data are from Table 1. The rare earth data are from (*1*) for north of 60°N and from J.-G.S. (unpublished) for south of 60°N; the Sr data are from (*4*). Note the broken scales south of 60°N. Crosses are for data from (*13*) and (*14*), the latter corrected for interlaboratory bias. $(\mathrm{La/Sm})_{\mathrm{EF}}$ stands for ratio of La and Sm enrichment factors relative to chondrite meteorite concentrations.

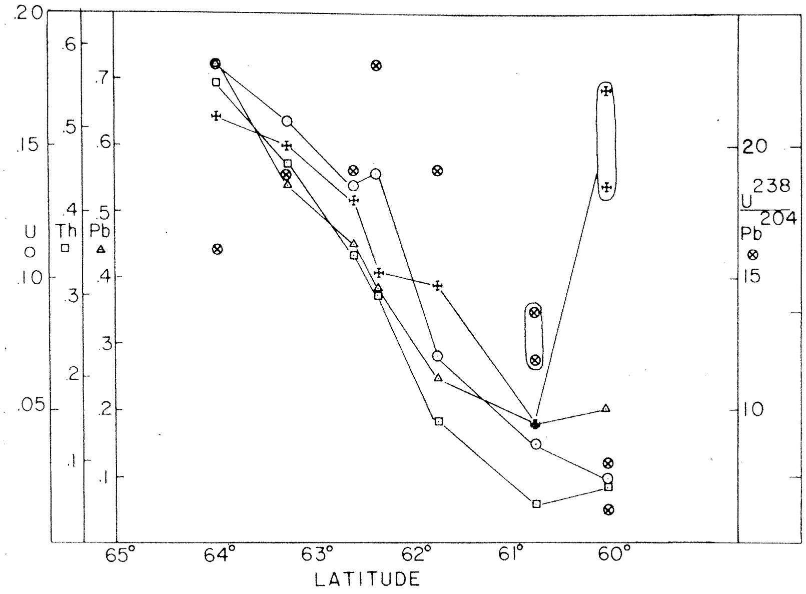

Fig. 3. Variation with latitude of U, Th, and total Pb concentrations (in parts per million) along the transitional zone of the Reykjanes Ridge; nearly linear profiles are observed. Variations in $^{238}U/^{204}Pb$ and $^{232}Th/^{238}U$ are also shown.

tween, in the transition zone, a two-step gradient is apparent. However, a case can be made that the envelope containing the statistical scatter is slightly convex upward relative to single LIL element gradients (*1*, *9*). In general, the $^{206}Pb/^{204}Pb$ profile resembles the $^{87}Sr/^{86}Sr$ profile except for the two low $^{87}Sr/^{86}Sr$ values at 208 and 248 km (E and H in Fig. 1), which are not correlated with similarly low $^{206}Pb/^{204}Pb$ values. The constant $^{206}Pb/^{204}Pb$, $^{208}Pb/^{204}Pb$, and La/Sm levels south of 61°N up to the Gibbs fracture zone, a stretch of some 1000 km, should also be noted in Fig. 2. A plot of the $^{207}Pb/^{204}Pb$ against distance, using the data of Table 1, would show a profile similar to those shown in Fig. 2, but with more scatter because of the greater uncertainty in $^{207}Pb/^{204}Pb$ measurements relative to the small range of variation observed.

Figure 3 shows the U, Th, Pb, $^{238}U/^{204}Pb$, and $^{232}Th/^{238}U$ variations along the ridge for seven samples from the transitional zone, except for the southernmost station, and one sample from the Reykjanes Peninsula. For 440 km (up to ~61°N) U, Th, and Pb decrease southward fairly regularly and then seem to level off, although U keeps decreasing (sample TR41-19D). The trend of U, Th, and Pb is similar to that of La or other LIL elements (*1*, *9*). However, these seven samples were selected for analyses on the basis of their La/Sm values. They represent samples that were closest to a first-order best fit to the La/Sm variation for some 34 samples previously reported by Schilling (*1*). The regularity is therefore not very surprising; nonetheless, it does confirm the highly coherent LIL trace element variation along the Reykjanes Ridge.

The $^{232}Th/^{238}U$ ratio in Fig. 3 also regularly decreases from 0 to 440 km (61°N), as would be anticipated from other LIL element ratios (*1*, *9*). However, rather than leveling off south of 61°N, the ratio for sample TR41-19D at 60°N shows, in duplicate analyses, an anomalously high value. The anomaly is due to a fortuitous combination of a slightly high Th value and low U value compared to those observed at the station at 61°N and may reflect some unknown contaminant, which at such low concentrations (see Table 2) is not at all unlikely. Finally, the $^{238}U/^{204}Pb$ variation in Fig. 3 also tends to decrease southward but with considerably more scatter, perhaps reflecting the mobile nature of lead.

Table 1. Locations and Pb isotopic compositions of samples in this study. For the locations zero is taken at the southwest tip of the Reykjanes Peninsula and distance is positive southward. The letter code is for reference to Fig. 1.

Sample	Code	Location (km)	$^{206}Pb/^{204}Pb$	$^{207}Pb/^{204}Pb$	$^{208}Pb/^{204}Pb$
IC 17	A	-144	18.629	15.488	38.207
IC 58	B	- 18	18.777	15.502	38.387
TR 101-11D-2	C	78	18.680	15.495	38.284
TR 101-1D-2	D	176	18.665	15.502	38.262
TR 101-22D-1 a.	E	208	18.522	15.478	38.060
TR 101-22D-1 b.			18.516	15.486	38.104
TR 101-23D-1-6	F	210	18.674	15.479	38.229
TR 101-34D-6	G	221	18.521	15.487	38.090
TR 101-24D-6	H	248	18.466	15.466	38.017
TR 101-27D-7A	I	298	18.460	15.453	37.998
TR 41-46D-1	J	352	18.475	15.476	38.038
TR 101-29D-5B	K	390	18.349	15.466	37.926
TR 101-30D-10A	L	390	18.361	15.451	37.896
TR 101-31D-9C	M	440	18.217	15.447	37.794
TR 41-20D-3 a.	N	543	18.288	15.463	37.821
TR 41-20D-3 b.			18.283	15.471	37.880
TR 41-19D	O	544	18.259	15.443	37.820
GLJ-10	P	660	18.195	15.449	37.725
TR 100-26D-11	Q	860	18.205	15.453	37.778
GLJ-7	R	1415	18.289	15.445	37.778

Test of binary mantle mixing model. It has been widely accepted that during partial melting in the mantle Pb and Sr isotopes are homogenized, and that subsequent fractional crystallization does not affect the isotopic ratios of such heavy elements if it occurs over a short period (< 5 million years) and without crustal contamination. In the absence of any compelling evidence to the contrary, and on this premise, Pb isotopic ratios (and $^{87}Sr/^{86}Sr$) in basalts along the Reykjanes profile should reflect the composition of the mantle source, or sources, of the basalts and the extent of mixing that took place if only two sources were involved. This should be true whether mixing occurred between the two different mantle sources (i) before melting, when they were solids; (ii) during partial melting, when they were crystal mushes; or (iii) subsequently, between segregated melts, provided the mixing took place on a short time scale. Thus, isotopic ratios can be more reliable than data for single LIL elements for testing the mixing model, since LIL element concentrations are subject to variation during partial melting and fractional crystallization. Naturally, some information is lost if only isotopic compositions are considered, and the detailed genesis of these basalts can be unraveled only by simultaneously considering variations in individual LIL element concentrations, LIL element ratios, and major elements trends along the ridge (*12*). However, in this report we limit ourselves to demonstrating that mixing of two mantle sources indeed appears to have taken place.

Various tests are available using combinations of the three lead isotopic ratios,

^{206}Pb/^{204}Pb, ^{207}Pb/^{204}Pb, and ^{208}Pb/^{204}Pb, and, to a more limited extent, total Pb, U, and Th. Three main types of tests are now considered.

Table 2. Uranium, thorium, and lead concentrations, ^{232}Th/^{238}U, and ^{238}U/^{204}Pb for selected samples. The letter code is for reference to Fig. 1. The K_2O percentages (by weight) are from (*1*); ppm, parts per million.

Sample	Code	K_2O (%)	Concentration (ppm) U	Th	Pb	Atomic ratios ^{232}Th/^{238}U	^{238}U/^{204}Pb
IC 58	B	0.25	0.180	0.552	0.722	3.17	15.9
TR 101-11 D2	C	0.20	0.159	0.459	0.540	2.99	18.7
TR 101-1D-2	D	0.20	0.135	0.347	0.449	2.67	19.1
TR 101-23D-1-6	F	0.22	0.139	0.299	0.384	2.22	23.1
TR 101-27D-7A	I	0.11	0.0700	0.145	0.246	2.14	19.1
TR 101-31D-9C	M	0.06	0.0385	0.0488	0.176	1.31	13.7
TR 101-31D-9C			0.0355	0.0450	0.188	1.31	11.7
TR 41-19D	N	0.04	0.0211	0.0682	0.207	3.34	6.41
TR 41-19D			0.0252	0.0674	0.198	2.76	7.98

1) The most direct test of the binary mantle mixing model is to plot one isotopic ratio against another. A linear correlation should be obtained regardless of the sample location along the ridge if only two end members of constant isotopic composition were involved in the mixing. A linear correlation should also be obtained when any elemental ratio is plotted against another if only mixing were involved. Figure 4, a and b, shows plots of ^{208}Pb/^{204}Pb and ^{207}Pb/^{204}Pb, respectively, against ^{206}Pb/^{204}Pb. Both diagrams show a good degree of linear correlation, which suggests binary mixing, but this is not an entirely unequivocal interpretation as such regression lines have been interpreted otherwise (*15*). However, a plot of Th/U against La/Sm is also a straight line (Fig. 4c). This suggests that partial melting had little influence and that crystal fractionation was not effective in masking the linear correlation expected for binary mixing. These results are not unexpected as tholeiitic basalts represent relatively large degrees of partial melting of mantle peridotites. Over such a range of partial melting the ratios for LIL elements, which have crystal/melt partition coefficients much less than unity, become practically identical to those in their mantle source, and the variations of these ratios are not very sensitive to fluctuations in the extent of partial melting (*16*). Furthermore, as pointed out by Gast (*17*) and Schilling (*6, 18*), LIL trace element ratios are not much affected by olivine gabbro fractionation at shallow depth, over a range consistent with maintaining an overall tholeiitic basalt chemistry.

2) Another test for binary mixing is to plot lead isotopic ratios against the inverse of the total lead concentration. Ideally a linear relationship should result, as shown by Lancelot and Allegre (*19*)—again regardless of the sample location along the ridge. Figure 4d shows such a plot for the Reykjanes Ridge. The expected linearity for binary mixing is confirmed for all three lead isotopic ratios. Variations in lead concentrations produced by differences in degree of partial melting and extent of subsequent crystal fractionation at shallow depth could have been expected to partly mask the mantle mixing correlation. However, these two effects appear to have been negligible. Using the intercept value for ^{206}Pb/^{204}Pb in Fig. 4d (18.94) and Lancelot and Allegre's formula (*19*), we calculate R_A = 18.75 and 38.36 for the ^{206}Pb/^{204}Pb and ^{208}Pb/^{204}Pb ratios for the Iceland end member mantle source, beneath the Median Neovolcanic Zone. Both values correspond to the highest value obtained over the area and thus are consistent with the binary mixing model. However, the Th/U ratios of corresponding Iceland basalts (3 to 3.3) are too low to support growth of ^{208}Pb in a closed system for 4.6 billion years from a primordial Pb isotopic ratio. This was also noted by Hart *et al.* (*4*) for the Rb/Sr-^{87}Sr/^{86}Sr system and by Tatsumoto (*20*) for oceanic tholeiites. Thus, in some sense the mantle beneath the Median Neovolcanic Zone is already partly depleted and does not represent primordial material.

3) Another test is to determine the variation of the Iceland mantle contribution (Z) to the mixture as a function of distance (l) along the ridge from various geochemical gradients and to obtain a best fit for $Z = f(l)$ from all the data available. A full account of such a treatment will be given elsewhere (*21*). It is sufficient to point out here that for binary mixing, the Sr or Pb isotopic ratio (R_M) of the mixture is a function not only of the isotopic ratios of the two end-member sources (R_A and R_B), as is the case for any single-element concentrations, but also of the total Pb (or Sr) concentrations of the two end members, C_A and C_B (*20*). Thus, a plot of R_M as a function of the relative mixing proportions (Z), which in a first approximation vary regularly and decrease southward along the ridge, is usually a parabola, with a curvature dependent on the value of the parameter n (that is, C_A/C_B). This is also true for LIL element ratios (*21*). The model predicts curves that are convex upward for the variation along the ridge of Pb and Sr isotopic ratios—and to a lesser extent Th/U and La/Sm ratios (because of the low value of n for U and Sm in particular)—whereas straight lines should be obtained for single LIL elements if only binary mixing was involved. It also predicts a pronounced convex downward curve for

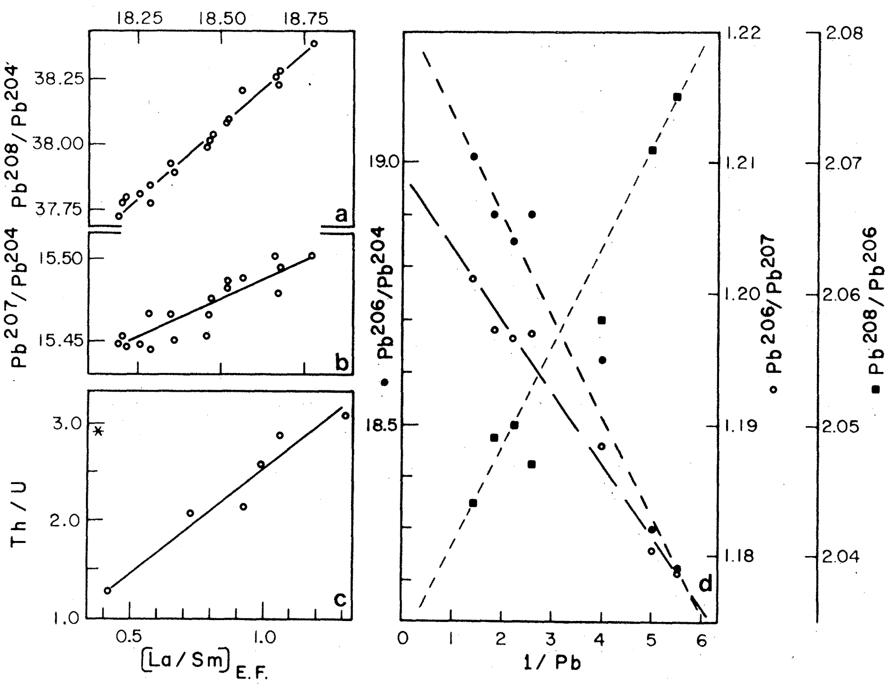

Fig. 4. Tests of the binary mixing model. In (c) the asterisk is for the anomalous sample TR41-19D. All the plots show the linearity expected for a binary mixing model.

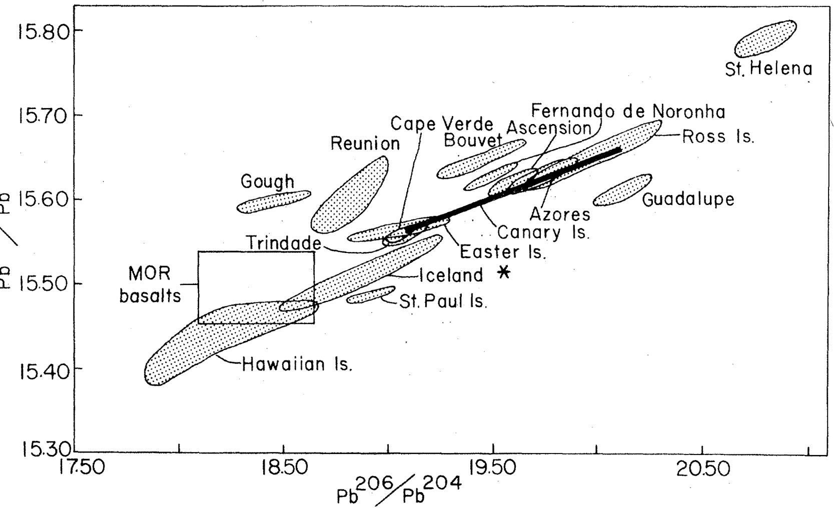

Fig. 5. Lead isotopic ratios in volcanic rocks of oceanic islands and mid-oceanic ridge (*MOR*) basalts. Note that many of the island trends point toward Pb isotopic values of MOR basalts. Data are from Sun (*11*), except for Iceland (*13*). Iceland (asterisk) data do not include the Reykjanes Ridge data presented here.

the U/Th profile along the ridge because of the high value of *n* for Th. Figure 2 [see also figure 2 in (*1*)] and a plot of U/Th with relevant data from Table 2 indicate good first-order agreement with the model. This satisfactorily explains (i) the tendency of the high PB and Sr isotopic ratios from Iceland to extend farther south on the submerged Iceland platform than do single LIL elements, which begin decreasing immediately from the southwestern border of Iceland; and (ii) the relatively more abrupt change southward of ^{87}Sr/^{86}Sr and, to a lesser extent, Pb isotopic ratios—a change which otherwise might be interpreted to suggest less extensive mixing.

In summary, all tests of mixing using U, Th, total Pb, and Pb isotopes in various combinations have been consistent with the binary mantle plume mixing model originally proposed for explaining the variations in rare earth element abundances along the Reykjanes Ridge (*1*).

Alternative Models. First, alternative models involving a single mantle source, such as those postulating increasing fractional crystallization or decreasing partial melting toward Iceland, could quantitatively explain portions of the geochemical data along the Reykjanes Ridge. However, Schilling has shown that the amount of fractional crystallization (*6*) and the range of partial melting (*1*) required to quantitatively match the gradients of LIL ratios are too great to be consistent with a tholeiitic basalt chemistry along the entire profile. Furthermore, both models would predict eruptions of smaller volumes of lavas over Iceland, either as residual magmas or produced by smaller degrees of partial melting, than are observed for Iceland relative to the Mid-Atlantic Ridge (*1, 22*).

Second, O'Nions and Pankhurst (*7, 23*), Sigvaldason *et al.* (*8*), and Flower *et al.* (*24*) have invoked disequilibrium partial melting to explain the ^{87}Sr/^{86}Sr variations and the LIL element ratios. The hypotheses suggest that melts can have higher or lower ratios of radiogenic isotopes than the mantle source from which they are derived. The radiogenic isotope ratios of the melt are a function of the degree of melting, in a way that depends on the mineral phases invoked for the mantle, the radiogenic isotope ratios of the minerals before melting, the order and rates of melting of the mineral phases, and their extent of isotopic disequilibrium relative to the melt. To be considered seriously, such disequilibrium models would have to be qualitatively and quantitatively developed so as to simultaneously satisfy the Pb and Sr isotopic data observed along the Iceland-Reykjanes profile, as well as the linear relations shown in Figs. 3 and 4. So far, these models have not been developed in this way.

Finally, the possibility of contamination of basalts from southwestern Iceland by crustal material richer in radiogenic Pb and Sr appears to be ruled out on at least two grounds. First, the uniformity of ^{87}Sr/^{86}Sr ratios in basalt across Iceland (*4*), speaks against an irregular process such as contamination. Second, the spatial and temporal variation of Pb and Sr isotopes in Icelandic volcanism (*7, 13*) appears inconsistent with contamination. Although there is a positive covariant relationship between Pb and Sr isotopes (*4*) along the postglacial Iceland-Reykjanes profile, the Iceland tertiary basalts are less radiogenic in Pb (*13, 14*) but more radiogenic in Sr isotopes (*25*) and richer in light rare earths (*26*) than are postglacial tholeiitic basalts from southwestern Iceland. Thus, contamination by migration of postglacial tholeiitic basalt melts through tertiary lava piles could not have produced results consistent with the observed spatial and temporal variations of both radiogenic Pb and Sr.

Conclusions.

1) The binary mantle mixing model proposed by Schilling (*1*) has been tested against Pb isotopic data and more limited Th, U, and Pb concentration data and is consistent with these data.

2) The Pb isotopic data do not rule out increasing extents of fractional crystallization at shallow depth and partial melting toward Iceland. Both effects are, in fact, independently suggested by the trends in single LIL elements and the more subdued major element profiles (*12*). However, they do not seem to have been extensive enough to mask the linear correlation expected for binary mixing in plots of Pb isotopic ratios against 1/Pb (Fig. 4d), Th/U against La/Sm (Fig. 4c), and U/Th against distance. In other words, mixing appears to have been the dominant process responsible for the observed gradients of isotopic and LIL element ratios, whereas the subdued gradients for major elements and only a small fraction of the LIL element enrichments are caused by crystal fractionation at shallow depth and fluctuations in partial melting along the profile (*9, 12*).

3) A dynamic mixing process, such as upwelling of one mantle source relative to another, could have effectively produced the Pb isotopic mixing required along the transitional zone. Our data do not directly prove the existence of a plume [or blob (*26*)] which rises beneath Iceland and then mixes by overflowing into the low velocity zone beneath the ridge. However, we consider the geophysical and morphological evidence discussed by Vogt and others (*27*) and Schilling (*1*), together with our data, to be sufficient evidence to support this model.

4) Finally, to conclude and further suggest the probable impact of the Iceland-Reykjanes Ridge mixing model, we note that a plot of ^{207}Pb/^{204}Pb against ^{206}Pb/^{204}Pb for many oceanic islands astride or near the mid-oceanic ridge (MOR) system shows linear trends pointing toward values for the normal MOR basalts (Fig. 5). Such lines have generally been interpreted in terms of a two-stage model age (*15*). We suggest that such linear trends may have been produced by mixing that occurred when small mantle plumes (apparently isotopically different from one another) became contaminated with depleted low velocity layer mantle material while penetrating the asthenosphere from below. Entirely consistent with this interpretation is

the overwhelming evidence that the depleted low velocity layer mantle source of normal ridge basalts is, to a first approximation, uniform in space and time and practically worldwide in extent (*16, 18, 20*), whereas mantles feeding oceanic islands appear to be different from one another in both rare earth and isotopic composition (*28*) and seem to have been derived from greater depths and to cover only limited areas of the oceans (*1, 29*).

SHINE-SOON SUN
Lamont-Doherty Geological Observatory of Columbia University, New York 10964, and
Department of Earth and Space Sciences, State University of New York, Stony Brook 11794

MITSUNOBU TATSUMOTO
U.S. Geological Survey, Denver, Colorado 80225

JEAN-GUY SCHILLING
Graduate School of Oceanography, University of Rhode Island, Kingston 02881

References and Notes

1. J.-G. Schilling, *Nature (Lond.)* **242**, 565 (1973).
2. J. T. Wilson, *ibid.* **197**, 536 (1963).

→ W. J. Morgan, *ibid.* **230**, 42 (1971).

4. S. R. Hart, J.-G. Schilling, J. L. Powell, *ibid.* **246**, 104 (1973).
5. M. J. O'Hara, *ibid.* **243**, 507 (1973).
6. J.-G. Schilling, *ibid.* **246**, 141 (1973).
7. R. K. O'Nions and R. J. Pankhurst, *Earth Planet. Sci. Lett.* **21**, 13 (1973).
8. G. E. Sigvaldason, S. Steinthorsson, N. Oskarsson, P. Imslad, *Nature* (*Lond.*) **251**, 579 (1974).
9. S. R. Hart and J.-G. Schilling, *Carnegie Inst. Wash. Yearb.* **72**, 259 (1973).
10. The analyses were carried out at the Denver laboratory of the U.S. Geological Survey and at the State University of New York at Stony Brook. In both cases a solid source, double focusing, 12-inch-radius mass-spectrometer of the National Bureau of Standards type, equipped with a magnetic stabilizer and computerized data acquisition system, was used. Lead samples were analyzed by the phosphate–silica gel method. The NBS 982 standard Pb was routinely measured to monitor the mass-fractionation correction. The data reported here are believed to be accurate within ± 0.1 percent for $^{206}Pb/^{204}Pb$. Concentrations of U, Th, and Pb were determined by isotopic dilution by M.T., using 1-g samples in a clean laboratory. The Pb blanks during these analyses ranged from 1.5 to 3 ng.
11. M. Tatsumoto, *J. Geophys. Res.* **71**, 1721 (1966); ———, R. J. Knight, M. H. Delevaux, *U.S. Geol. Surv. Prof. Pap. 800-D* (1972), p. 111; S. S. Sun, thesis, Columbia University (1973).
12. J.-G. Schilling and O. D. Hermes, in preparation.
13. S. S. Sun and B. M. Jahn, *Nature* (*Lond.*) **255**, 527 (1975).

→ H. Welke, S. Moorbath, G. L. Cumming, H. Sigurdsson, *Earth Planet. Sci. Lett.* **4**, 221 (1968).

15. For example, see T. J. Ulrych, *Science* **158**, 252 (19 → R. D. Russell, W. F. Slawson, T. J. Ulrych, P. H. Reynolds, *Earth Planet. Sci. Lett.* **3**, 284 (1967).
16. J.-G. Schilling, *J. Geophys. Res.* **80**, 1459 (1975).
17. P. W. Gast, *Geochim. Cosmochim. Acta* **32**, 1057 (1968).
18. J.-G. Schilling, *Philos. Trans. R. Soc. Lond. Ser. A Math. Phys. Sci.* **268**, 663 (1971).
19. J. R. Lancelot and C. J. Allegre, *Earth Planet. Sci. Lett.* **22**, 233 (1974). Their equation of mixing is

$$R_M = \frac{1}{C_M}\frac{C_A C_B(R_A - R_B)}{C_A - C_B} + R_B + (R_A - R_B)\frac{C_A}{C_A - C_B}$$

where R_A, R_B, and R_M are any Pb isotopic ratios in mantle sources A and B and the mixture, respectively, and C_A and C_B are the total concentrations of lead in A and B, respectively. To calculate R_A from the intercept, we used $R_B = 18.25$, the average value south of 61°N (a good estimate). On a relative basis, we estimated $C_A/(C_A - C_B)$ by using the average Pb concentration of the basalt over the Median Neovolcanic Zone of Iceland [0.702 part per million (ppm)] and south of 61°N (0.202 ppm); we assumed the same degree of partial melting, so the effect would be canceled out as it appears in both on numerator and denominator.

20. M. Tatsumoto, *Science* **153**, 1094 (1966).
21. J.-G. Schilling, in preparation. The equation for binary mixing is approximately

$$Z = \frac{(R_B - R_A)}{R_M(n - 1) - (nR_A - R_B)}$$

where Z is the mass ratio of component mantles A/A + B; R_A, R_B, and R_M were defined in (*19*); and $n = C_A/C_B$. Then Z can be solved for various R_M values for radiogenic isotope ratios or LIL element ratios observed along the transitional part of the ridge. This dependence for isotopic ratios was independently noted by J. Cann, East Anglia University, and communicated to J.-G.S.

22. G. E. Sigvaldason, *J. Petrol.* **15**, 497 (1974).
23. R. K. O'Nions and R. J. Pankhurst, *ibid.*, p. 603.
24. M. F. J. Flower, H. U. Schmincke, R. N. Thompson, *Nature (Lond.)* **254**, 404 (1975).
25. R. K. O'Nions and R. J. Pankhurst, *Earth Planet. Sci. Lett.* **21**, 13 (1973).
26. J.-G. Schilling, unpublished rare earth data for eastern Iceland; see also ——— and A. Noe-Nygaard, *Earth Planet. Sci. Lett.* **24**, 1 (1974).
27. P. R. Vogt, *Earth Planet. Sci. Lett.* **13**, 153 (1971); ——— and G. L. Johnson, *ibid.* **18**, 49 (1973); P. R. Vogt, in *Geodynamics of Iceland and the North Atlantic Area*, L. Kristjansson, Ed. (Reidel, Boston, 1975), p. 105.
28. For example, see (*11*); P. W. Gast, *Phys. Earth Planet. Interiors* **3**, 296 (1970); Z. E. Peterman and C. E. Hedge, *Geol. Soc. Am. Bull.* **82**, 493 (1971); C. E. Hedge, N. D. Watkins, R. A. Hidreth, W. P. Doering, *Earth Planet. Sci. Lett.* **21**, 29 (1973).
29. J.-G. Schilling, D. G. Johnson, T. H. Johnston, *Trans. Am. Geophys. Union* **55**, 294 (1974); J.-G. Schilling, *Earth Planet. Sci. Lett.* **25**, 103 (1975).

30. Supported in part by NSF grant DES 72-01705.

24 June 1975

Flooding Frequency of Hypersaline Coastal Environments Determined by Orbital Imagery: Geologic Implications

Abstract. *Available satellite imagery in the infrared and near-infrared wavelengths provides a simple, rapid, and low-cost method for monitoring the extent and duration of the flooding of coastal ecosystems. Hypersaline environments in Baja California, Mexico, are flooded as a result of complex interactions between the higher of the two spring tides each month and local winds. Such flooding necessitates a reappraisal of ideas on rhythmic lamination in algal mats, stromatolites, and evaporite sediments preserved in the geologic record.*

One of the persistent problems confronting researchers in coastal processes has been the lack of repetitive data for periods of several years with observation intervals of 1 month or less. This is particularly true for remote locations. Earlier investigators of lagoons, supratidal regions, and adjacent salt flats (*1*) have reported the need for synoptic coverage of the frequency and duration of flooding of these coastal environments. Fluctuations in the areal extent of standing water contribute to the total water budget in the area and aid one in understanding subsurface refluxing and evaporation-humidity parameters. Satellite imagery, primarily the near-infrared band of LANDSAT-1 (Land Satellite) [formerly called ERTS-I (Earth Resources Technology Satellite)], in combination with field observations, is being successfully employed in our work in Baja California, Mexico, to fill this gap in previous investigations.

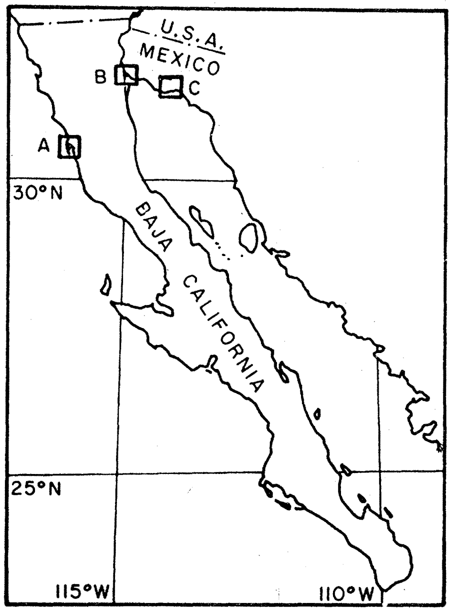

Fig. 1. Location of hypersaline deposits in Baja California, Mexico; site A, Laguna Mormona; site B, Salina Ometepec; site C, Salina Grande (Sonora).

Because infrared wavelengths penetrate water to a depth of only a few centimeters, there is a sharp contrast between water-covered surfaces and adjacent surfaces. On the basis of an analysis of the near-infrared band (0.8 to 1.1 μm) of the LANDSAT-1 multispectral scanner imagery, using a binocular microscope for zoom magnification, we were able to separate a given location (for example, the northern gypsum flat at Laguna Mormona; Fig. 1), into three classes based on a quantitative optical gray scale: (i) black, standing water; (ii) medium to dark gray, moist area; and (iii) light gray to white, dry ground. The areal percentage of each type of surface was then determined. Water bodies on the evaporite flats as small as 150 m in diameter were detectable. The technique we developed is similar to that of Reeves (*2*) who used a density control unit calibrated to a photo-